Full Paper

Applied Organometallic Chemistry

Received: 29 April 2009 Revised: 14 May 2009 Accepted: 20 May 2009 Published online in Wiley Interscience: 26 June 2009

(www.interscience.com) DOI 10.1002/aoc.1522

Synthesis, characterization and oxygen-sensing properties of a novel luminescent Cu(I) complex

Linfang Shi[a], Bin Li[b]*, Shaozhe Lu[b], Dongxia Zhu[b] and Wenlian Li[b]

A novel luminescent copper(I) complex with formula $[Cu(PPh_3)_2(PIP)]BF_4$ (PPh_3 = triphenyl phosphine, PIP = 2-phenyl-1*H*-imidazo[4,5-*f*][1,10]phenanthroline) has been synthesized and characterized by ^1H NMR, IR, elemental analysis and X-ray crystal structure analysis. In solid state, it displays broad band emission upon excitation at λ = 420 nm with the emission maximum locates at 551 nm. Its excited-state lifetime is in the microsecond time scale (3.02 μs); as a result, its emission intensity is sensitive to oxygen concentration and shows oxygen-sensing properties after being encapsulated into mesoporous silica MCM-41. For the system with 60 mg/g loading level, a sensitivity (I_0/I) of 4.35, a fluorescence quenching time (t_Q) of 5 s and a recovery time (t_R) of 36 s were achieved. Even after aging for 5 months, the sensitivities of the three loading level systems can be retained, ignoring the measurement error, which indicates that they possess long-term stability.

Keywords: luminescence; X-ray diffraction; copper(I) complex; oxygen-sensing

Introduction

In the past decades, luminescent copper(I) complexes have attracted special attention due to the low cost of the metal and lesser toxicity of the complexes.[1] Many efforts have been made to explore applications of copper(I) complexes in solar energy conversion, biological probing and organic light-emitting diodes.[2] Luminescence-based oxygen-sensing is another important application for luminescent metal complexes because the determination of oxygen concentration in gaseous, aqueous samples and biological fluids has great significance. Oxygen is a powerful quencher of the emission intensity and excited state lifetime of some luminescent complexes. Many metal complexes have been tested as oxygen-sensing probes and some of them displayed excellent performance.[3] However, few reports on the application of copper complexes in oxygen-sensing have been published so far.[4]

In order to examine the possibility of practical application of complexes based on this inexpensive metal in oxygen sensing, we synthesized a novel luminescent copper(I) complex $[Cu(PPh_3)(PIP)]BF_4$ and studied its photophysical and oxygen-sensing properties. For practical applications in optical oxygen-sensing devices, it is necessary to incorporate the dye molecules into a solid matrix that can act as a medium for supporting the dye molecules and for oxygen transportation from the environment. There are many reports on luminescence-based oxygen sensor utilizing different matrixes,[3f,5] from which it can be concluded that the support indeed has quite stringent criteria for suitable performance. Additionally, for a suitable matrix, it must lend itself to a convenient attachment to the sensor probe. Mesoporous silica are able to physically encapsulate and immobilize the probe molecules in the pores; furthermore, the existence of channels in these materials allows transportation of small molecules including molecular oxygen into the mesoporous silica. Therefore the luminescence of probe molecules incorporated in the silica could be quenched readily by oxygen molecules surrounding it.

For the reasons mentioned above, we chose mesoporous silica Mobil Catalytic Material 41(MCM-41) as the matrix because it possesses high surface area and periodic nanoscale pores, which facilitate the adsorption and desorption of oxygen. We have conventionally encapsulated this copper(I) complex into the well-studied mesoporous silica MCM-41 by physical incorporation technique and tested its oxygen-sensing properties. The results of the experiments indicate that $[Cu(PPh_3)(PIP)]BF_4$ displays oxygen-sensing properties being incorporated into such matrix. Compared with sensors based on noble metal complexes, application of Cu(I) complex doped composite material in oxygen-sensing is environmentally friendly and economically attractive.

Experimental

Synthesis of PIP and Complex

$[Cu(PPh_3)(PIP)]BF_4$(PIP = 2-phenyl-1*H*-imidazo[4,5-*f*][1,10]phenanthroline) was synthesized according to reported procedures.[6a,b] Complex $[Cu(PPh_3)(PIP)]BF_4$ was synthesized following a similar procedure reported in the literature.[6c] To a 100 ml

* *Correspondence to: Bin Li, Changchun Institute of Optics, Fine Mechanics and Physics, Chinese Academy of Sciences, Key Laboratory of Excited-State, Changchun 130033, People's Republic of China. E-mail: lib020@yahoo.cn*

a *College of Science, Zhejiang Forestry University, Linan 311300, People's Republic of China*

b *Key Laboratory of Excited State Processes, Changchun Institute of Optics, Fine Mechanics and Physics, Changchun 130033, People's Republic of China*

flask was added $[Cu(CH_3CN)_4]BF_4$ (31 mg, 0.1 mmol), PPh_3 (52 mg, 0.2 mmol) and dichloromethane (10 ml), and stirred for 1 h. Then PIP (30 mg, 0.1 mmol) was added and stirred for another hour. After the evaporation of solvent, the product was obtained as a yellow powder. Yield: 80 mg (70%). ^{1}H NMR (300 MHz, $CDCl_3$, 25 °C): δ = 9.352 (d, J = 6.0 Hz, 2H), 8.652 (d, J = 5.4 Hz, 2H), 8.457 (d, J = 6.0 Hz, 2H), 7.745 (m, 2H), 7.614 (m, 2H), 7.469 (m, 1H), 7.376 (m, 2H), 7.314 (m, 5H), 7.289 (m, 4H), 7.224 (m, 12H), 6.987 (m, 5H), 6.799 (m, 2H) ppm. Anal. calcd for $C_{55}H_{42}BCuF_4N_4P_2$ (971.26): C, 68.02; H, 4.36; N, 5.77. Found: C, 68.04; H, 4.34; N, 5.79. IR (KBr pellet): ν 3053, 1619, 1435, 1058, 747 cm^{-1}.

Preparation of Mesoporous Silica MCM-41 and the Corresponding Complex/MCM-41 System

MCM-41 was synthesized according to reported procedures with some minor modifications.[7] $[Cu(PPh_3)_2(PIP)]BF_4$/MCM-41 (40, 60 and 80 mg/g) composite systems were prepared by the following procedure. In a typical preparation, $[Cu(PPh_3)_2(PIP)]BF_4$ (4 mg) was dissolved in 10 ml dichloromethane, then MCM-41 (0.1 g) was added to the solution and kept stirring for 24 h at room temperature, filtered. The obtained powder was washed with solvent and then dried in the air; finally the target composite material was obtained. Samples with different loading levels (40, 60 and 80 mg/g) were prepared by altering the concentration of initial solution of $[Cu(PPh_3)_2(PIP)]BF_4$.

Spectroscopy

IR spectrum was acquired using a Magna560 FT-IR spectrophotometer. Element analysis was performed using a Vario Element Analyzer. The ^{1}H NMR spectrum was obtained using a Varian INOVA 300 spectrometer. UV–vis absorption spectra were recorded using a Shimadzu UV-3101PC spectrophotometer. All of the photoluminescence (PL) spectra were measured with a Hitachi F-4500 fluorescence spectrophotometer. The photoluminescence quantum yield of $[Cu(PPh_3)_2(PIP)]BF_4$ is defined as the number of photons emitted per photon absorbed by the system and was measured with an integrating sphere by a literature method.[8] Luminescent lifetimes were obtained with a 355 nm light generated from the Third-Harmonic-Generator pump, which used a pulsed Nd–YAG laser as excitation source. The Nd : YAG laser possesses a line width of 1.0 cm^{-1}, pulse duration of 10 ns and repetition frequency of 10 Hz. A Rhodamine 6G dye pumped by the same Nd–YAG laser was used as the frequency-selective excitation source. Powder small angle X-ray diffraction (SAXRD) data were collected on a Bruker D8 Discover diffractometer equipped with Cu target (λ = 1.5406 ´Å). The scanning range was 1–10° with a 0.01° step and scanning speed was 1 s/step. All measurements were carried out in the air at room temperature without being specified.

Crystallography

A single crystal of $[Cu(PPh_3)_2(PIP)]BF_4{\cdot}C_2H_5OH$ suitable for X–ray diffraction studies was grown from slow evaporation of C_2H_5OH-CH_2Cl_2 solution. The crystal was measured on a Bruker Smart Apex CCD single-crystal diffractometer using λ(Mo KR) radiation, 0.7107 Å at 273 K. An empirical absorption was based on the symmetry-equivalent reflections and applied to the data using the SADABS program. The structure of $[Cu(PPh_3)_2(PIP)]BF_4{\cdot}C_2H_5OH$ was solved using SHELXL-97 program.[9] Its crystallographic refinement parameters are summarized in Table 1, while selected bond distances and angles are given in Table 2 (CCDC 729210).

Table 1. Crystal data and structure refinement for $[Cu(PPh_3)_2(PIP)]BF_4{\cdot}C_2H_5OH$

Formula	$C_{57}H_{48}BCuF_4N_4OP_2$
Fw	1017.33
T (K)	273(2)
Wavelength (Å)	0.71 073
Crystal system	Triclinic
Space group	$P-1$
a (Å)	10.2354(16)
b (Å)	14.536(2)
c (Å)	18.379(3)
α (deg)	94.040(2)
β (deg)	104.177(2)
γ (deg)	106.893(2)
V (Å)	2507.2(7)
Z	2
ρ_{calcd} (mg/m^3)	1.300
μ (mm^{-1})	0.556
F(000) (e)	1016
Crystal color	Yellow
Crystal size (mm)	0.397 × 0.306 × 0.211
Range of transmission factors (deg)	2.15–26.10
Reflections collected	21 751
Unique	9867
Completeness to θ = 26.06	99.0%
Data/restraints/params	9867/0/631
GOF on F^2	0.781
R_1, wR_2 [$I > 2\sigma(I)$]	0.0558, 0.0995
R_1, wR_2 (all data)	0.1370, 0.1190

Table 2. Selected bond lengths (Å) and angles (deg) for $[Cu(PPh_3)_2(PIP)]BF_4{\cdot}C_2H_5OH$[a]

N(1)–Cu(1)	2.081(3)
N(2)–Cu(1)	2.084(3)
P(1)–Cu(1)	2.2805(12)
P(2)–Cu(1)	2.2658(12)
N(1)–Cu(1)–N(2)	80.00(13)
N(1)–Cu(1)–P(2)	111.33(9)
N(2)–Cu(1)–P(2)	114.09(9)
N(1)–Cu(1)–P(1)	109.10(9)
N(2)–Cu(1)–P(1)	109.64(9)
P(2)–Cu(1)–P(1)	124.02(4)

[a] Numbers in parentheses are estimated standard deviations in the least significant digits.

Oxygen-sensing Properties Test

The oxygen-sensing properties of our samples were discussed based on luminescence intensity quenching instead of excited-state lifetime because it is hard to obtain precise excited-state lifetime values with a conventional flashlamp-based time-correlated photon counting system.[10] Excitation wavelength of all samples was 420 nm. In the measurement of Stern–Volmer plots, oxygen and nitrogen were mixed at different concentrations via gas flow controllers and passed directly to the sealed gas chamber. We typically allowed 1 min between changes in N_2/O_2 concentration to ensure that a new equi-

librium point had been established. Equilibrium was evident when luminescence intensity remained constant. Sensor response curves were obtained using a similar method. The experiments were carried out in the dark at room temperature.

Results and Discussion

Synthesis and Characterization

Complex $[Cu(PPh_3)_2(PIP)]BF_4$ was prepared according to a reported method with some modifications.[6c] It was characterized by ^1H NMR, elemental analysis and IR. Aromatic protons of PPh_3 in $[Cu(PPh_3)_2(PIP)]BF_4$ appeared as complex sets of multiplets (some overlapping) in the region $\delta = 7.376$ to $\delta = 6.799$ ppm. The existence of PPh_3 molecule was further confirmed by the IR spectrum of the complex: absorption located at 1435 cm^{-1} is a characteristic vibration of P–Ar. The presence of aryl groups in the complex was confirmed by absorptions located at 747 and 3053 cm^{-1}, which should be attributed to out-of-plane deformations of C–H and stretching vibrations of =C–H, respectively. Absorption located at 1619 cm^{-1} was attributed to C=N stretching vibrations. The presence of $[BF_4]^-$ anion was found in the IR spectrum with ν (B–F) mode at 1058 cm^{-1}.[6c]

For further confirmation of its molecular structure, single crystals of $[Cu(PPh_3)_2(PIP)]BF_4 \cdot C_2H_5OH$ were selected for X-ray diffraction analysis. Single-crystal X-ray structure determinations of $[Cu(PPh_3)_2(PIP)]BF_4 \cdot C_2H_5OH$ show that copper(I) ion was in a N2P2 distorted tetrahedral environment in which two PPh_3 molecules were bound through their pair of P donor atoms, and PIP ligand through two diimine N atoms. Crystal data and refinement details for $[Cu(PPh_3)_2(PIP)]BF_4 \cdot C_2H_5OH$ are presented in Table 1. ORTEP representation of its structure is shown in Fig. 1, while selected bond length and bond angles are given in Table 2. It is clear from the data summarized in Table 2 that bond lengths of Cu–N and those of Cu–P are within the normal range.[1e,f,6c] The distortion presumably arises from the restricted bite angle of PIP ligand N(1)–Cu(1)–N(2), which is 80.00°, whereas the corresponding diphosphine bite angle P(1)–Cu(1)–P(2) is 124.02°.

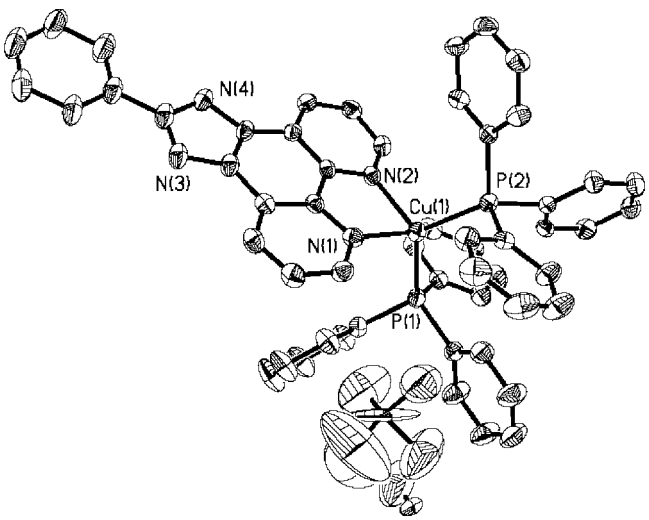

Figure 1. ORTEP drawing of crystal of $[Cu(PPh_3)_2(PIP)]BF_4 \cdot C_2H_5OH$ with displacement ellipsoids at the 30% probability level. Hydrogen atoms are omitted for clarity.

Photophysical Properties

As shown in Fig. 2, the absorption spectrum of $[Cu(PPh_3)_2(PIP)]BF_4$ recorded in CH_2Cl_2 exhibits intense $\pi-\pi^*$ ligand-centered bands in the region of 220–350 nm and weak and broad metal-to-ligand charge-transfer (MLCT) bands with an onset at 450 nm. The absorption maximum in visible region locates at 405 nm.

In air-equilibrated CH_2Cl_2 solution, $[Cu(PPh_3)_2(PIP)]BF_4$ exhibited no luminescence, which is similar to [Cu(DPEphos)(1,10-phenanthroline)]BF_4.[6c] In solid state, it exhibited luminescence from MLCT excited states. Upon excitation at $\lambda = 420$ nm, it displayed broad band emission with λ_{max} located at 551 nm (Fig. 3). Its solid-state photoluminescence quantum yield measured according to reported method was 0.08.[8] As shown in Fig. 4, its PL spectrum was composed of two exponential decays and the values were on the order of microseconds.

Oxygen-sensing Properties

The oxygen-sensing properties of $[Cu(PPh_3)_2(PIP)]BF_4$ were tested by physically incorporating it into mesoporous silica MCM-41 (designated as complex/MCM-41) with three loading levels of 40, 60 and 80 mg/g, respectively. The sensitivity properties of our present samples are discussed on the basis of luminescence intensity quenching.

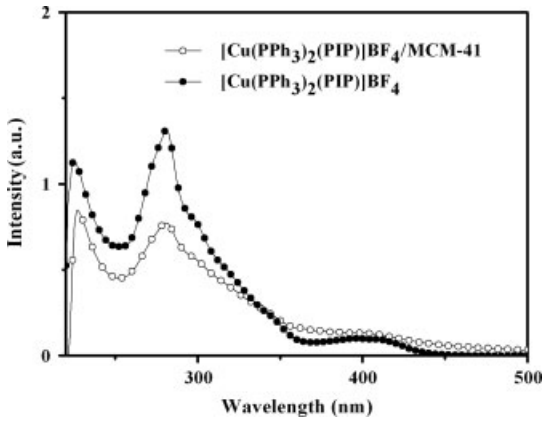

Figure 2. UV–vis absorption spectra of $[Cu(PPh_3)_2(PIP)]BF_4$ and $[Cu(PPh_3)_2(PIP)]BF_4$–MCM-41 (60 mg/g) composite material in dichloromethane solution.

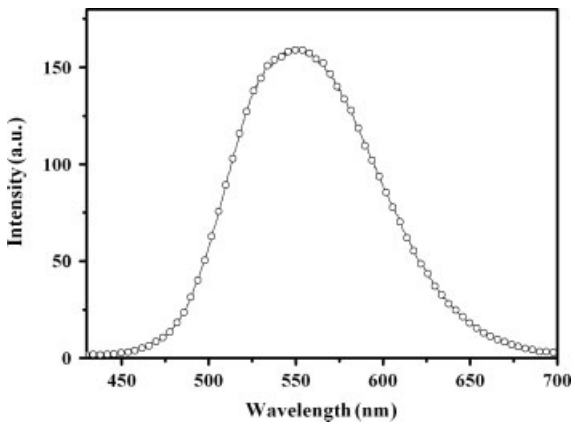

Figure 3. Emission spectrum of $[Cu(PPh_3)_2(PIP)]BF_4$ in solid state.

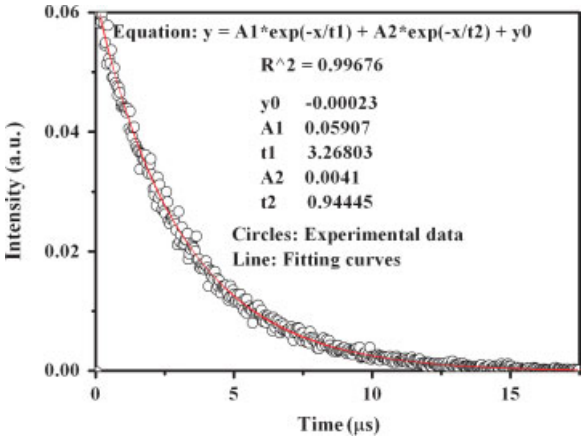

Figure 4. Solid-state photoluminescence lifetime decay curve of $[Cu(PPh_3)_2(PIP)]BF_4$ in the air.

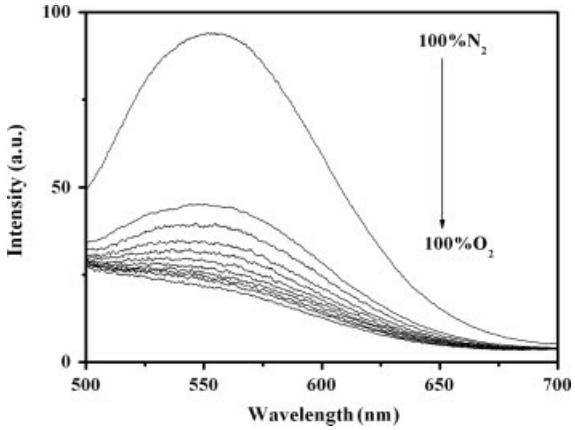

Figure 6. Emission spectra of $[Cu(PPh_3)_2(PIP)]BF_4$/MCM-41 (60 mg/g) under different oxygen concentrations.

As can be seen from Fig. 5, powder small-angle X-ray diffraction (SAXRD) measurements reveal that blank MCM-41 shows three well-resolved broad Bragg reflections that can be indexed as d_{100}, d_{110} and d_{200}, which are characteristic of a well-ordered hexagonal mesostructure.[11] SAXRD spectra (Fig. 5) of the composite materials display an identical pattern to that of MCM-41, indicating that the hexagonal arrangement of channels in MCM-41 is retained after the incorporation of $[Cu(PPh_3)_2(PIP)]BF_4$. The absorption spectra of the composite materials in dichloromethane are essentially the same as that of $[Cu(PPh_3)_2(PIP)]BF_4$ (Fig. 2). For clarity, only the spectrum of the 60 mg/g system is given in Fig. 2. All of the three loading level systems exhibit characteristic emission of $[Cu(PPh_3)_2(PIP)]BF_4$. Emission spectra of a 60 mg/g loading level system under different oxygen concentrations are presented in Fig. 6.

Stern–Volmer plots shown in Fig. 7 are nonlinear within a wide range of oxygen concentrations. The nonlinearity of the Stern–Volmer plots in our present work indicates the presence of heterogeneity in the composite system. This phenomenon can be explained by the fact that the luminophore molecules are distributed simultaneously between two or more sites within silica support in which one site is more heavily

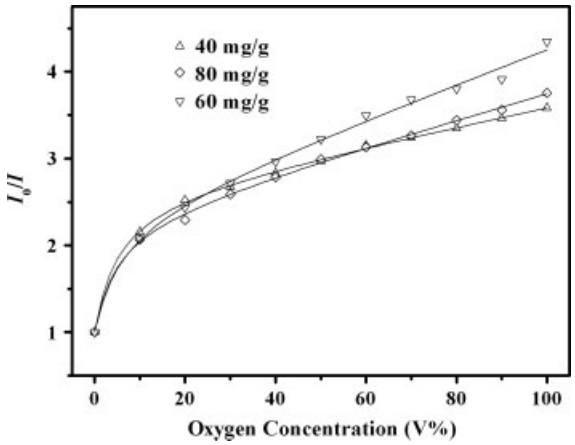

Figure 7. Stern–Volmer plots for $[Cu(PPh_3)_2(PIP)]BF_4$/MCM-41 systems at different oxygen concentrations. The solid lines are the best fits using Demas model.

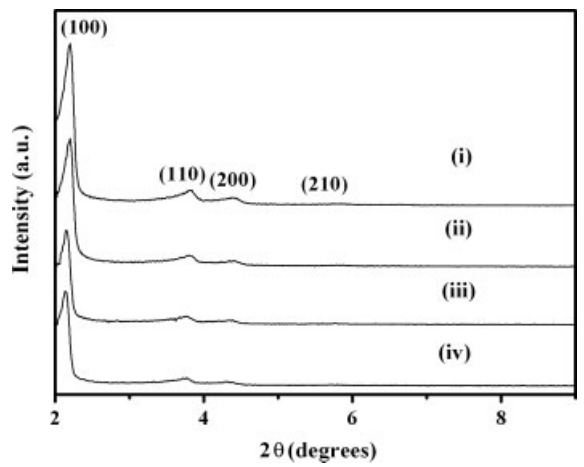

Figure 5. Powder X-ray spectra of MCM-41 (i) and $[Cu(PPh_3)_2(PIP)]BF_4$/MCM-41 with the loading levels of 40 (ii), 60 (iii) and 80 mg/g (iv).

quenched than the others. As a result, the ideal Stern–Volmer equation[10,12]

$$I_0/I = 1 + K_{SV}pO_2 \quad (1)$$

which is used in the ideal homogeneous environment is not suitable for these nonlinear Stern–Volmer plots because different microheterogeneous sites exhibit different quenching constant K_{SV} values. In this case, the idealized eqn (1) can be recast as[13]

$$\frac{I_0}{I} = \left[\sum_{i=1}^{m} \frac{f_i}{1 + K_{SVi}\, pO_2}\right] \quad (2)$$

where f_i is the fractional contribution from each oxygen accessible site, and K_{SVi} is the associated Stern–Volmer quenching constant for each accessible site. In microheterogeneous solids-based oxygen sensing systems, at low oxygen concentration, easily accessible luminescence molecules are quenched more effectively, whereas quenching responses at high oxygen concentrations are increasingly dominated by the less accessible domains.[14] If only two primary luminophore sites exist in the matrix, eqn (2) can be derived as:

$$\frac{I_0}{I} = \frac{1}{\dfrac{f_{01}}{1 + K_{SV1}\, pO_2} + \dfrac{f_{02}}{1 + K_{SV2}\, pO_2}} \quad (3)$$

Table 3. Values of t_Q, t_R, sensitivity (I_0/I_{100}) and Demas model[a] oxygen-quenching fitting parameters for three loading level systems

Loading level (mg/g)	t_Q (s)	t_R (s)	I_0/I_{100}	$K_{SV1}(O_2\%^{-1})$	$K_{SV2}(O_2\%^{-1})$	f_{01}[b]	R^2
40	4	60	3.58	0.49 796	0.00 391	0.62 887	0.99 936
60	5	36	4.35	0.47 608	0.0062	0.58 706	0.99 859
80	5	45	3.75	0.40 468	0.0079	0.60 502	0.99 601

[a] Terms are from eqn (3). [b] $f_{01} + f_{02} = 1$.

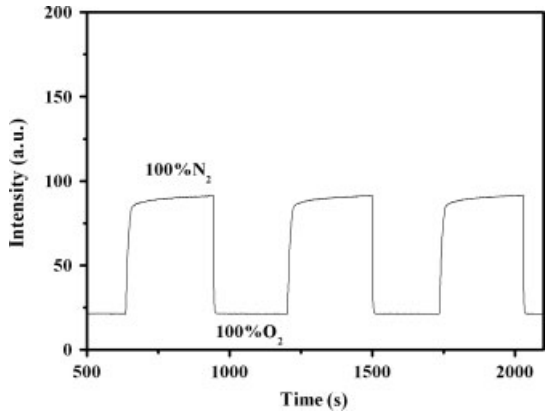

Figure 8. Response time and relative intensity change of $[Cu(PPh_3)_2(PIP)]BF_4$/MCM-41 (60 mg/g) to alternate environments of 100% nitrogen and 100% oxygen.

Equation (3) is the familiar Demas 'two-site' model that has been proved to have excellent ability to fit the downward turning of the Stern–Volmer plots.[10,13,14] The results of nonlinear fitting are compiled in Table 3, from which it can be seen that the Demas model is applicable to our data.

Quenching time (t_Q) and recovery time (t_R)[3h] are also very important parameters in evaluating an oxygen sensor. Response property tests were carried out on all of the samples and values of t_Q and t_R are displayed in Table 3. For clarity, only the response curve of 60 mg/g loading level system is presented (Fig. 8). It can be observed that recovery times are longer than response times for the three loading level samples. This phenomenon has been rationalized by the fact that the oxygen molecule is well known to be adsorbed strongly on the silica surface, and the long recovery time may be attributed to slow desorption of oxygen from silica surface in the support.

Values of sensitivity (I_0/I_{100}, where I_0 and I_{100} represent luminescent intensities in 100% nitrogen and 100% oxygen, respectively) of the samples are also given in Table 3. Complex $[Cu(PPh_3)_2(PIP)]BF_4$ incorporated into MCM-41 with 60 mg/g loading level shows higher sensitivity than those of 40 and 80 mg/g levels, which indicates that 60 mg/g is optimal. This fact can be explained as follows. There are at least two opposite factors affecting sensitivity of the samples: emission intensity from the probe molecules and adverse interaction between them (aggregation, for example). When the loading level is low, emission from probe is comparatively weak, which will result in low sensitivity; when it is high, aggregation between the probe molecules in the pores of the support may become serious. The two opposite factors mentioned above probably affect sensing properties of composite systems simultaneously; as a result, the highest sensitivity was achieved in the 60 mg/g system.

Conclusions

A novel luminescent copper(I) complex $[Cu(PPh_3)_2(PIP)]BF_4$ was synthesized and characterized. It displays oxygen-sensing properties being incorporated into mesoporous silica MCM-41. It is environmentally and economically attractive, employing comparatively inexpensive and nontoxic metal complexes in oxygen sensing.

Acknowledgments

The authors gratefully acknowledge the financial support of the One Hundred Talents Project from the Chinese Academy of Sciences and the NSFC (grant no. 50 872 130, 10 874 180).

References

[1] a) A. Lavie-Cambot, M. Cantuel, Y. Leydet, G. Jonusauskas, D. M. Bassani, N. D. McClenaghan, *Coord. Chem. Rev.* **2008**, *252*, 2572; b) N. Armaroli, G. Accorsi, F. Cardinali, A. Listorti, *Top. Curr. Chem.* **2007**, *280*, 69; c) D. R. McMillin, K. M. McNett, *Chem. Rev.* **1998**, *98*, 1201; d) N. Armaroli, *Chem. Soc. Rev.* **2001**, *30*, 113; e) D. V. Scaltrito, D. W. Thompson, J. A. O'Callaghan, G. J. Meyer, *Coord. Chem. Rev.* **2000**, *208*, 243; f) L. Yang, J. Feng, A. Ren, M. Zhang, Y. Ma, X. Liu, *Eur. J. Inorg. Chem.* **2005**, *10*, 1867; g) N. Armaroli, G. Accorsi, G. Bergamini, P. Ceroni, M. Holler, O. Moudam, C. Duhayon, B. Delavaux-Nicot, J. F. Nierengarten, *Inorg. Chim. Acta* **2007**, *360*, 1032.

[2] a) W. Jia, T. McCormick, Y. Tao, J. Lu, S. Wang, *Inorg. Chem.* **2005**, *44*, 5706; b) A. Tsuboyama, K. Kuge, M. Furugori, S. Okada, M. Hoshino, K. Ueno, *Inorg. Chem.* **2007**, *46*, 1992; c) Q. Zhang, Q. Zhou, Y. Cheng, L. Wang, D. Ma, X. Jing, F. Wang, *Adv. Mater.* **2004**, *16*, 432; d) S. Zhao, R. Wang, S. Wang, *Inorg. Chem.* **2006**, *45*, 5830.

[3] a) J. N. Demas, B. A. Degraff, *Coord. Chem. Rev.* **2001**, *211*, 317; b) S. M. Borisov, A. S. Vasylevska, C. Krause, O. S. Wolfbeis, *Adv. Funct. Mater.* **2006**, *16*, 1536; c) S. M. Borisov, O. S. Wolfbeis, *Anal. Chem.* **2006**, *78*, 5094; d) S. M. Borisov, V. V. Vasil'ev, *J. Anal. Chem.* **2004**, *59*, 155; e) S. H. Cheng, C. H. Lee, C. S. Yang, F. G. Tseng, C. Y. Mou, L. W. Lo, *J. Mater. Chem.* **2009**, *19*, 1252; f) B. Meier, T. Werner, I. Klimant, O. S. Wolfbeis, *Sens. Actuators, B, Chem.* **1995**, *B29*, 240; g) S. M. Borisov, G. Nuss, I. Klimant, *Anal. Chem.* **2008**, *80*, 9435; h) C. Huo, H. Zhang, H. Zhang, H. Zhang, B. Yang, P. Zhang, Y. Wang, *Inorg. Chem.* **2006**, *45*, 4735.

[4] a) M. T. Miller, T. B. Karpishin, *Sens. Actuators, B, Chem.* **1999**, *61*, 222; b) L. F. Shi, B. Li, S. M. Yue, D. Fan, *Sens. Actuators, B, Chem.* **2009**, *137*, 386.

[5] a) A. S. Kocincova, S. Nagl, S. Arain, C. Krause, S. M. Borisov, M. Arnold, O. S. Wolfbeis, *Biotechnol. Bioeng.* **2008**, *100*, 430; b) M. C. Moreno-Bondi, O. S. Wolfbeis, M. J. P. Leiner, B. P. H. Schaffar, *Anal. Chem.* **1990**, *62*, 2377; c) O. S. Wolfbeis, L. J. Weis, M. J. P. Leiner, W. E. Ziegler, *Anal. Chem.* **1988**, *60*, 2028.

[6] a) E. A. Steck, A. R. Day, *J. Am. Chem. Soc.* **1943**, *65*, 452; b) C. W. Jiang, H. Chao, R. H. Li, H. Li, L. N. Ji, *Polyhedron* **2001**, *20*, 2187; c) S. M. Kuang, D. G. Cuttell, D. R. McMillin, P. E. Fanwick, R. A. Walton, *Inorg. Chem.* **2002**, *41*, 3313.

[7] B. F. Lei, B. Li, H. R. Zhang, L. M. Zhang, W. L. Li, *J. Phys. Chem. C.* **2007**, *111*, 11291.

[8] M. S. Wrighton, D. S. Ginley, D. L. Morse, *J. Phys. Chem.* **1974**, *78*, 2229.

[9] a) G. M. Sheldrick, *SHELXTL, version 5.10*; Siemens Analytical X-ray Instruments Inc.: Madison, WI, **1998**; (b) *SMART and SAINT*; Siemens Analytical X-ray Instruments Inc.: Madison, WI, **1995**; (c) G. M. Sheldrick, *SADABS*. University of Göttingen: Göttingen, **1996**.
[10] B. Lei, B. Li, H. Zhang, Sh. Lu, Z. Zheng, W. Li, Y. Wang, *Adv. Funct. Mater.* **2006**, *16*, 1883.
[11] J. S. Beck, J. C. Vartuli, W. J. Roth, M. E. Leonowicz, C. T. Kresge, K. D. Schmitt, C. T-W. Chu, D. H. Olson, E. W. Sheppard, S. B. McCullen, J. B. Higgins, J. L. Schlenker, *J. Am. Chem. Soc.* **1992**, *114*, 10834.
[12] V. O. Stern, M. Volmer, *Physik. Zeitschr.* **1919**, *20*, 183.
[13] a) Y. Tang, E. C. Tehan, Z. Y. Tao, F. V. Bright, *Anal. Chem.* **2003**, *75*, 2407; b) W. Y. Xu, R. C. McDonough, B. Langsdorf, J. N. Demas, B. A. DeGraff, *Anal. Chem.* **1994**, *66*, 4133; c) E. R. Carraway, J. N. Demas, B. A. DeGraff, J. R. Bacon, *Anal. Chem.* **1991**, *63*, 337; d) J. N. Demas, B. A. Deora, W. Y. Xu, *Anal. Chem.* **1995**, *67*, 1377; e) J. R. Bacon, J. N. Demas, *Anal. Chem.* **1987**, *59*, 2780.
[14] B. W.-K. Chu, V. W. W. Yam, *Langmiur* **2006**, *22*, 7437.